ILASS–Europe 2022, 31th Conference on Liquid Atomization and Spray Systems, 6-8 September 2022, Virtual, Israell

Stretching separation in drop-jet collisions

David Baumgartner[1], Günter Brenn[1], Carole Planchette*[1]
[1]Institute of Fluid Mechanics and Heat Transfer, Graz University of Technology, 8010 Graz, Austria
*Corresponding author: carole.planchette@tugraz.at

Abstract
Motivated by the production of fibers and capsules via in-air microfluidics, we study the fragmentation of Newtonian and viscoelastic jets subjected to collisions with drops made of another immiscible liquid. For Newtonian liquids, the jet fragmentation is total and the mechanism is similar to the one observed during the stretching separation of two colliding drops. Considering the drop-jet collisions as a succession of off-centre drop-drop collisions, a model is established that predicts the jet fragmentation threshold as a function of the jet Ohnesorge number Oh_j, the drop Weber number We_d, and an adapted impact parameter $\tilde{X}$. For viscoelastic jet liquids, the stream of spherical capsules observed with Newtonian jets disappears. Instead, long-lived filaments emerge that connect the capsules creating what we call “Capsules-On-A-String” (COAS). We explain this phenomenon by the dramatic change of the filament drainage kinetics.

Keywords
Jet, Drop, Fragmentation, Viscoelastic, Stretching

Introduction

In various fields, such as agriculture, food, cosmetic, or pharmaceutical industries, active ingredients must be delivered in a controlled manner. This includes several aspects. For example: perfect dosing to ensure efficiency and safety, active protection to avoid degradation from the environment, specific targeting to reduce consumption and potential pollution, or tuning of the release kinetics to prolong or shorten the effects. In this context, liquid encapsulation is a strategy of choice. Established methods based on sprays or emulsions may not always provide the required level of control. Other approaches have important drawbacks such as high costs, low yields and, more specifically for microfluidics, important risks of clogging, which keep preventing its scale-up. In this challenging context, the usage of drop-jet collisions, also called in-air microfluidics, appears as a promising route [1,2]. It combines a very high degree of control (size, shape and composition of the capsules) with high yields (tens of kHz) and low costs (no need for expensive equipment). Furthermore, it eliminates the risk of clogging. The method, however, is rather new, and a better understanding of the different collision outcomes and the limits separating them is required to implement it in a rational way [3]. With this paper, we make a first step in this direction. More precisely, we focus on the fragmentation limit of the jet, which separates the following regimes: *drops-in-jet* and *capsules or capsules-on-a-string (COAS)*. The *drops-in-jet* corresponds to a continuous cylindrical liquid jet in which the droplets are regularly embedded, forming spherical inclusions made of the drop liquid. It is observed for both Newtonian and viscoelastic jet liquids and is illustrated by the picture of Figure 1a. By increasing the drop inertia or the drop spacing, the jet fragments. For Newtonian liquids, it leads to a stream of *capsules*, after which this type of outcome is named. Each capsule contains exactly one drop, as shown in Figure 1b. Finally, when the jet is viscoelastic, the jet fragmentation is delayed and partly suppressed, giving rise to *capsules-on-a-string*. This structure corresponds to a succession of capsules – containing

exactly one drop as previously defined - but connected by long lived filaments made of the jet liquid only, see Figure 1c. These results were obtained using immiscible liquids but they are expected to remain valid for miscible liquids. Indeed, as long as the jet surface tension is smaller than the one of the drops, the outcomes of drop-jet collisions with miscible and immiscible liquids are found to be similar. This can be understood by the fact that no significant mixing develops over the considered timescale [4].

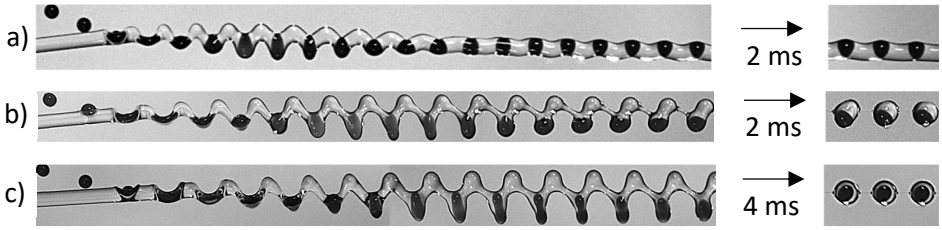

Figure 1: Drop-jet collisions (a) below and (b-c) above the jet fragmentation threshold. a) and b) Newtonian jet producing *drops-in-jet* and *capsules*, respectively. c) viscoelastic jet leading to *Capsules-On-A-String*. In all cases, the liquid jet is transparent while, the drops are dark.

To understand these behaviours and predict the limits between these three types of outcome, we make use of recent findings obtained for the stretching separation of two drops colliding off-center [5]. The paper is organized as follows. First, we introduce the problem parameters for both drop-drop and drop-jet collisions and explain the analogy between the two configurations. We then describe the experimental set-up and provide the properties of the studied liquids. With this framework, we show how the stretching separation model found for drop-drop collisions can be adapted to drop-jet collisions. We demonstrate the validity of this model using several Newtonian liquids and collision parameters and explain why it reaches its limits when viscoelastic jets are used. The paper ends with the conclusions.

Materials and Methods

- Problem parameters

The parameters introduced thereafter are all sketched in Figure 2. Throughout the paper, the subscripts d and j refer to the drops and jet (or their liquid), respectively. Considering drops of equal size, D_d and D_j are the drop and jet diameters with typical values of $190 < D_d < 370\ \mu m$ and $270 < D_j < 290\ \mu m$. The drops have a velocity $\vec{u}_d$ and are produced in the form of regular streams of periodicity L_d. The jet flow rate equivalent velocity is $\vec{u}_j$ and its periodicity L_j is defined as the distance separating two consecutive drop impacts, see also Figure 4d. For both drop-drop and drop-jet collisions, the relative velocity is denoted $\vec{U}$ and typically varies between 3 and $8\ m/s$. We only consider collisions for which the drop and jet trajectories are in the same plane. In the case of drop-jet collisions, we further limit our study to “normal” impacts, i.e. to collisions for which the relative velocity is perpendicular to the jet axis. In other words, we have: $\vec{U} \approx \overrightarrow{U_\perp}$ and $\overrightarrow{U_\parallel} \approx \vec{0}$, see Figure 2b.

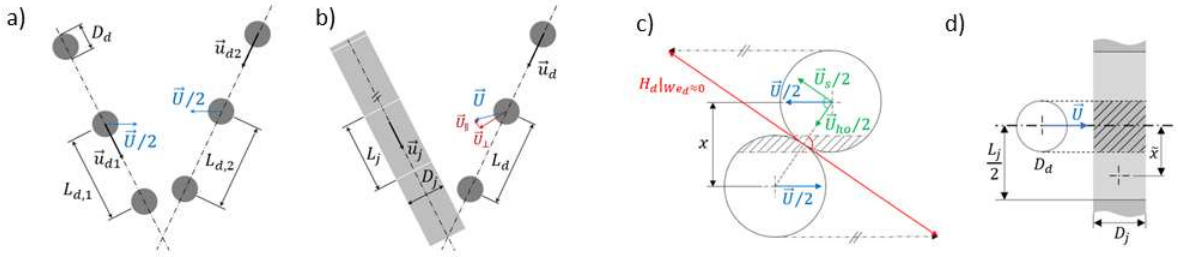

Figure 2: Sketches of (a) drop-drop and (b) drop-jet collisions. Definition of the impact parameter for (c) drop-drop collisions: parameter x and (b) drop-jet collisions: parameter $\tilde{x}$. Adapted from [5].

Finally, the eccentricity of the collision in its own plane must be characterized. This is done via the introduction of the impact parameter. For drop-drop collisions, we use the classical definition found in the literature, which corresponds to the distance separating the drop centers at contact after projection perpendicularly to the relative velocity, see Figure 2c. This impact parameter, x, is then normalized by the drop diameter to provide $X = x/D_d$. For drop jet-collisions, we associate the jet portion found directly behind the drop to the drop itself (hatched section in Figure 2d) and consider that this compound drop collides off-center with another drop, which corresponds to half the jet portion found between two consecutive drops (pale grey sections in Figure 2d). In this way, we obtain $\tilde{x} = (L_j + D_d)/4$. Since each compound drop interacts with two such portions, it must be counted twice before it is normalized by the jet diameter. This leads to the following normalized impact parameter $\tilde{X} = (L_j + D_d)/D_j$.

- Experimental set-up

To realize controlled drop-jet-collisions, we use the set-up depicted in Figure 3. More precisely, a drop generator and a nozzle are combined. They are mounted on micro-traverses to enable a fine adjustment of the drop and jet trajectories. The liquids are supplied by separate pressurized tanks to independently adjust the flow rates. To obtain regular drops, a piezo-crystal is excited at a known frequency denoted f_d. This frequency, typically ranging from 5 to $25\ kHz$, is also used to drive an LED system providing a stroboscopic illumination and thus standing pictures of the collisions. The collisions are recorded using two cameras placed parallel or perpendicular to the collision plane. While the parallel camera (denoted ∥) is mostly used to eliminate the eccentricity out of the collision plane, the perpendicular one (camera ⊥) provides the images that are analyzed to calculate all parameters mentioned in the previous section except $\vec{u}_j$. The latter is obtained by measuring the jet volume flow rate. Details about how to derive the parameters from the pictures can be found in [3-5].

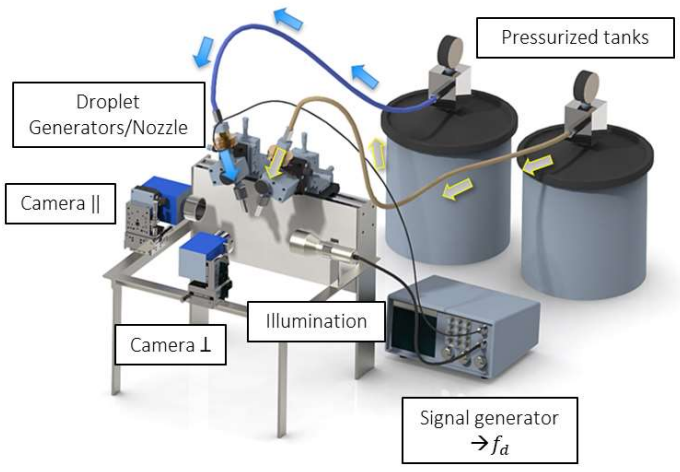

Figure 3: Experimental set-up used to obtain drop-jet collisions.

- Liquid properties

To complete the problem description, the liquid properties must be known. In this study, we combine an aqueous glycerol solution at 50%(w:w) for the drops (G5) with silicon based liquids for the jets and ensure in this way the total wetting of the drop liquid by the jet liquid. More precisely, we have four Newtonian silicon oils (SO-N) and two viscoelastic liquids based on silicon oils (SOED-M). They are obtained by mixing the silicon oils with different ratios of a silicon based elastomer (Elite Double 8 from Zhermack GmbH). More details can be found in

[6]. The liquids are then characterized in house. This includes the measurement of the density ρ, the surface and interfacial tensions σ, the zero shear viscosity μ and the relaxation time λ. The measurements are performed at room temperature (22 ± 2°C) using the established methods described in [6]. The results are gathered in Table 1. Note that in the abbreviation SO-N, N designates the zero shear viscosity in mPa.s while in SOED-M, M corresponds to the relaxation time in ms.

Table 1 – Liquid properties measured at room temperature.

	ρ (kg.m^{-3})	σ (mN.m)	μ (mPa.s)	λ (ms)
G5	1120 ± 5	68 ± 2	5.25 ± 0.15	-
SO-1	845 ± 3	18 ± 1	1.35 ± 0.10	-
SO-3	887 ± 5	18.5 ± 0.5	2.75 ± 0.10	-
SO-5	907 ± 5	19.5 ± 1	5.10 ± 0.10	-
SO-20	949 ± 5	20.5 ± 1	18.0 ± 0.5	-
SOED-1.3	945 ± 10	19.7 ± 1	19.0 ± 1.0	1.30 ± 0.15
SOED-2.5	900 ± 10	19.5 ± 1	16.5 ± 1.0	2.5 ± 0.1

Results and Discussion

- Stretching separation of Newtonian liquid jets

To understand the jet fragmentation limit observed for Newtonian drop-jet collisions, it is useful to first recall recent findings about the stretching separation found in binary drop collisions. One key point is that separation occurs when the merged drop is stretched beyond a certain critical value [5,7]. More precisely, fragmentation takes place when the normalized extension $\psi_d = H_d/D_d$, reaches a value of 3.25. Here H_d is the length of the stretched merged drop, see Figure 4a-b. The second important element to have in mind is that the evolution of ψ_d can be quantitatively described by the following equation:

$$\psi_d = 0.041\ {Oh_d}^{-0.13} X\ We_d + 2.7\ X + 0.5 \qquad (1)$$

Here $Oh_d = \mu_d/\sqrt{\rho_d \sigma_d D_d}$ is the drop Ohnesorge number, $We_d = \rho_d D_d U^2/\sigma_d$ the drop Weber number and X, the previously introduced normalized impact parameter [5]. The origin of the term $2.7\,X + 0.5$ is purely geometric and can be seen as a quasi-static contribution. It corresponds to the end-to-end distance of the merged drop projected along the stretching direction $\overrightarrow{U_s}$ (in contrast to the head-on direction $\overrightarrow{U_{ho}}$), see Figure 2c. It is represented in the same figure by the red line $H_d|_{We_d \to 0}$.The other term, proportional to ${Oh_d}^{-0.13} X\ We_d$, corresponds to the kinetic contribution of the almost undisturbed drop portions (not hatched in Figure 2c) corrected by the viscous loss taking place in the interacting volume (hatched in Figure 2c). The latter is estimated from the numerical results of Finotello et al. [8]. Practically, Equation (1) means that, for a given Oh_d, ψ_d increases linearly with We_d and the associated slope, $\partial\psi_d/\partial We_d$, increases linearly with X.

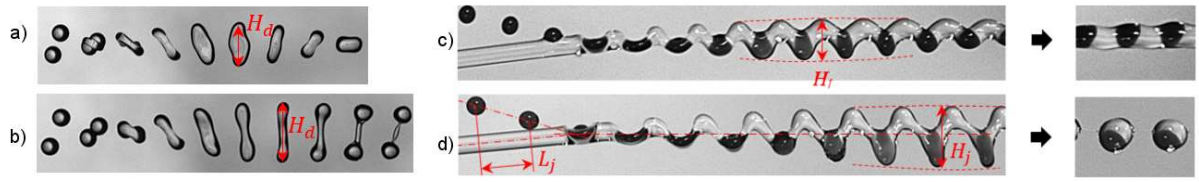

Figure 4: Drop-drop collisions with (a) $\psi_d < 3.25$ leading to coalescence and (b) $\psi_d > 3.25$ resulting in drop separation. Drop-jet collisions with (c) $\psi_j < 3.0$ proving *drops-in-jet* and $\psi_j > 3.0$, which produces *capsules*.

for drop-drop collisions, we observe that the jet fragments if its normalized maximal extension

$\psi_j = H_j/D_j$, exceeds a given critical value of 3.0. In this case, H_j represents the maximal extension of the stretched jet, measured in the collision plane, perpendicularly to its final trajectory, see Figure 4c-d. As shown by Figure 5a, where ψ_j is plotted as a function of We_d for various $\tilde{X}$, the critical value of 3.0 (horizontal dashed line) distinguishes very well *drops-in-jet* (full symbols) from *capsules* (empty symbols). These results are obtained for G5 (drops) and SO-20 (jet) with $D_j = D_d = 280\ \mu m$, which correspond to the jet Ohnesorge number, $Oh_j = \mu_j/\sqrt{\rho_j \sigma_j D_j}$, of 0.246 and a diameter ratio $\Delta = D_d/D_j$ of 1.0. Additional experiments performed with other silicon oils and various drop and jet diameters covering $0.021 < Oh_j < 0.246$ and $0.7 < \Delta < 1.3$ produce similar results (not shown) and validate the usage of $\psi_j = 3.0$ as a fragmentation criterion for Newtonian jets. Even more remarkable, the variation of ψ_j with We_d is linear, and the slope, $s_j = \partial\psi_j/\partial We_d$, increases linearly with $\tilde{X}$, see Figure 5b. These findings demonstrate the validity of the analogy between drop-jet and drop-drop collisions and therefore calls for the adaptation of Equation (1) to the present geometry. Assuming that the viscous losses now take place in the jet liquid, we replace the drop Ohnesorge number by the one of the jet. Thus the inertia-viscous term is expected to be proportional to ${Oh_j}^n \tilde{X}\, We_d$. Furthermore, we consider that, in contrast to drop-drop collisions, the deformation of geometric origin is modulated by Oh_j. This can be understood as the result of a competition between interfacial and bulk deformation, whose respective typical timescales are given by $\mu_j D_j/\sigma_j$ and $\sqrt{{\rho_j D_j}^3/\sigma_j}$, forming a ratio equal to Oh_j [9]. Consequently, we search for a function $\psi_{j,mod}$ of the following form :

$$\psi_{j,mod} = \alpha_j {Oh_j}^n \tilde{X}\, We_d + \beta_j\, {Oh_j}^n \tilde{X} + \gamma_j \qquad (2)$$

where $\alpha_j, \beta_j, \gamma_j$ and n are adjustable parameters.
Letting our experimental results be fitted by Equation (2), we obtain a very good agreement with $\alpha_j = 0.0066$, $\beta_j = 3.98$, $\gamma_j = -5.85$ and $n = -0.10$, see Figure 5c.

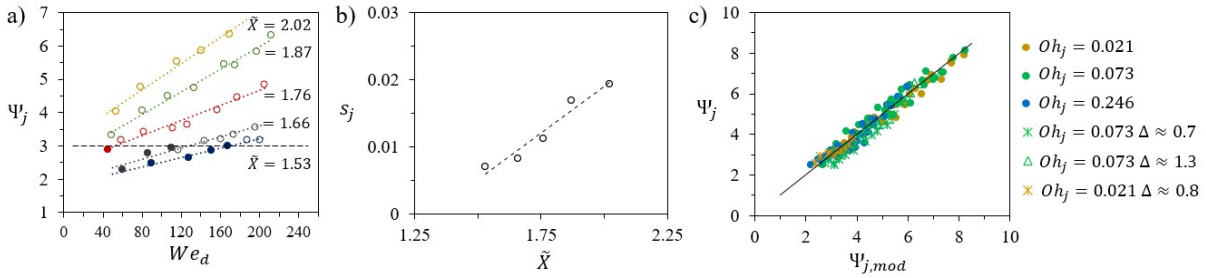

Figure 5: a) ψ_j as a function of We_d for different $\tilde{X}$ using SO-20 and G5 for the drop and jet liquids, respectively ($Oh_j = 0.246$ and $\Delta = 1.0$). Full (empty) symbols correspond to *drops-in-jet* (*capsules*) and the horizontal dashed line marks $\psi_j = 3.0$. b) Linear variation of s_j with $\tilde{X}$ (obtained from the data of (a)). c) Experimental measurements of ψ_j versus $\psi_{j,mod}$, the model given by Equation (2). Adapted from [5].

The limit of fragmentation is then simply obtained by combining the fragmentation criterion given by $\psi_j = 3.0$ with the theoretical prediction of the jet extension given by Equation (2). As expected, the results are very satisfactory for broad ranges of parameters ($0.021 < Oh_j < 0.246$ and $0.7 < \Delta < 1.3$) and advantageously replace the commonly used but imprecise criterion of $L_j/D_j \approx 2.0$, see Figure 6.

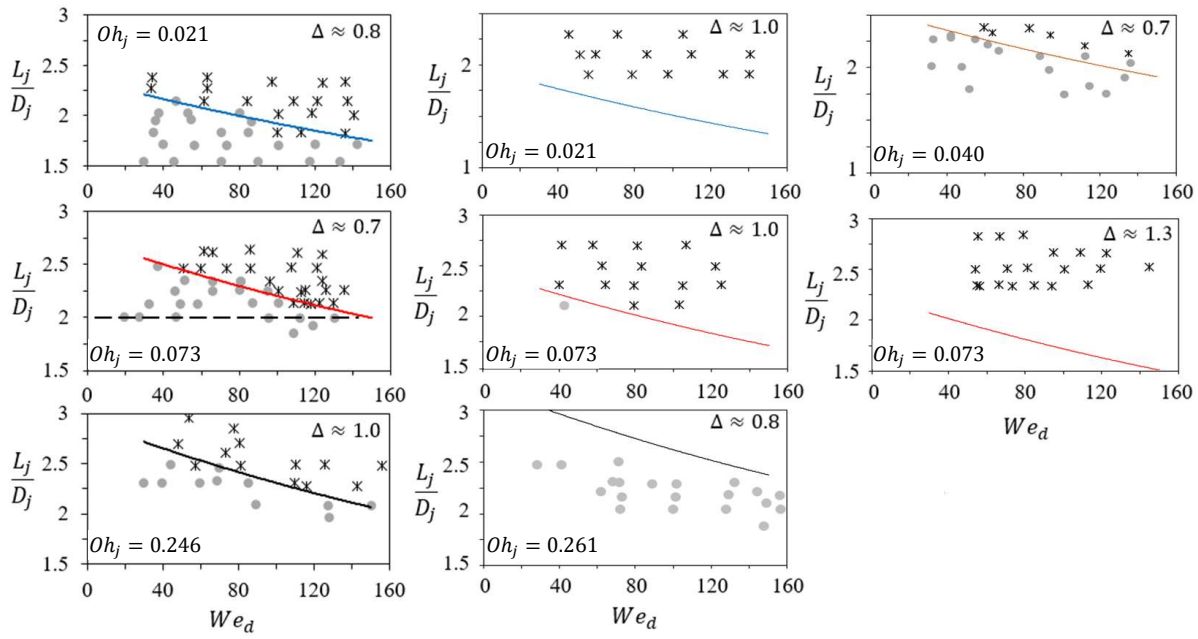

Figure 6: Regime maps of drop-jet collisions. Circles: *drops-in-jet* and stars: *capsules*. The continuous lines correspond to the limits predicted by combining Equation (2) with the fragmentation criterion $\psi_j = 3.0$. The dashed line represents the approximate limit given by $L_j/D_j \approx 2.0$.

- Long lived filaments of viscoelastic liquid jets

At this stage, it is legitimate to question the validity of our fragmentation model, especially when employing viscoelastic jets, since such liquids are well known to stabilize jets and suppress satellite drop formation. After having verified that, during the first instants following the collisions, the viscoelastic jets undergo comparable deformations as the Newtonian ones (see Figure 1b-c), we systematically measure ψ_j. We then plot for the two studied viscoelastic liquids, the data obtained as a function We_d for various values of $\tilde{X}$. The results are shown in Figure 7. As for Newtonian jets, the variation of ψ_j with We_d is linear and the slope, $s_j = \partial\psi_j/\partial We_d$, increases with $\tilde{X}$. Yet, the fragmentation criterion, namely the critical value of $\psi_j = 3.0$ does not separate *drops-in-jet* (full symbols) from *capsules*. Indeed, the capsules are replaced by *COAS* (empty symbols) and the transition is shifted to larger values of ψ_j (at least 3.2 for SOED-1.3 and 4.0 for SOED-2.5).

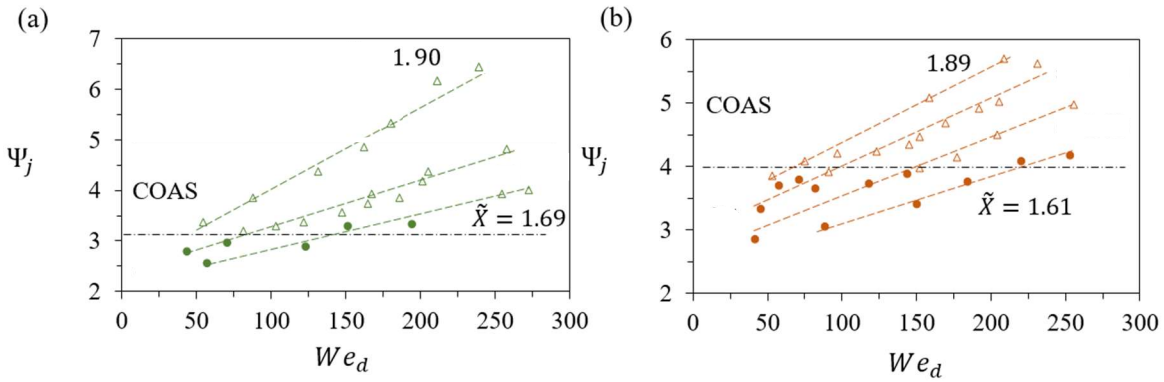

Figure 7: ψ_j as a function of We_d for different $\tilde{X}$ using (a) SOED-1.3 and (b) SOED-2.5 in combination with G5 for the drops. Circles: *drops-in-jet,* and empty symbols: *COAS*. The horizontal dashed lines mark the transitions between these two types of outcome. Adapted from [6].

We attribute the emergence of *COAS*, at the expense of simple *capsules*, to the change of drainage kinetics of the liquid filaments forming after collision. In the case of Newtonian liquids, the drainage, capillaro-viscous by nature, takes place over a typical timescale $t_N = \mu_j D_j/\sigma_j$, which is, for the studied liquids, in the order of $O(10^{-5}s)$ to $O(10^{-4}s)$. This timescale is short compared to the recoil time of the compound jet, typically scaling as $t_R = \sqrt{\rho_j {D_j}^3/\sigma_j} = O(10^{-3}s)$. As a consequence, if the collisions produce unstable filaments whose aspect ratio is greater than π or a value close to it [10], they will fragment before the compound jet has recoiled. If we further assume that ψ_j gives a first order estimation of the aspect ratio of the filaments forming upon collisions, ψ_j is expected to be an effective fragmentation criterion for Newtonian jets subjected to drop collisions. This interpretation is in agreement with the above reported findings showing that $\psi_j = 3.0$ separates *drops-in-jet* from *capsules*. In the case of viscoelastic liquids, the capillary drainage of the resulting liquid filaments is considerably slowed down by the elastic contribution at stake [11]. It typically takes the form of an exponential decay whose timescale is given by the liquid relaxation time. Having in mind that, in the present study, the relaxation times are comparable to t_R, one understands that the viscoelastic filaments generated by the collisions do not have enough time to complete their drainage before the overall structure recoils. Consequently, *COAS* form instead of *capsules*. Beyond the development of these long lived filaments, we also observe the extension of the *drops-in-jet* domain toward greater values of ψ_j. In other words, the conditions required to obtain *drops-in-jet*, i.e. stable filaments, are not the same for Newtonian jets ($\psi_j < 3.0$) and viscoelastic ones (up to $\psi_j = 4.0$). This cannot solely be explained by the change of drainage kinetics, which only modifies how quickly unstable filaments may eventually fragment. We suspect that the elasticity of the jet liquid, and more particularly the increased value of its extensional viscosity, leads to different deformation. Indeed, despite similar early appearance, we cannot exclude changes in the overall shape of the stretched sections. Thus, similar values of ψ_j could lead to filaments of different aspect ratios and explain why the transition is shifted toward greater values of ψ_j. While a complete understanding of this phenomenon requires further investigation, it is already possible to practically take advantage of it to favor the formation of *drops-in-jet* and thus the production of advanced fibers.

Conclusions

In the view of employing drop-jet collision to encapsulate liquids it is essential to predict the jet fragmentation limit. Adapting recent findings on the stretching separation of colliding drops, we develop a model that predicts this limit very well as long as Newtonian jet liquids are used. In this case, the fragmentation criterion corresponds to an excessive extension of the jet stretched by the collisions. The model only requires the knowledge of the jet Ohnesorge number Oh_j, the drop Weber number We_d, and the impact parameter $\tilde{X}$, which can be deduced from the collision geometry. It is valid over a wide range of collision parameters without any adjustment. Yet, when viscoelastic jet liquids are employed, the model cannot be used anymore. First, the *capsules* are replaced by *capsules-on-a-string*, also called *COAS*. This can easily be explained by the emergence of long lived viscoelastic filaments. Second, the transition between *drops-in-jet* and *COAS* does not occur for the same excessive jet extension as for Newtonian liquids. We suspect the elastic stress at stake to modify the geometry of the stretched structure and thus to affect its recoil and stability. Practically, the elastic stabilization of the jet can be used to favour the formation of *drops-in-jet* and thus to extend the parameter space associated to advanced fiber production.

Acknowledgments

We would like to acknowledge the financial support received from the Austrian Science Fund (FWF, grant P31064-N36) and from Austria Wirtschaftsservice Gesellschaft mbH (promotional bank of the Austrian federal government, grant P1910259-WTG01).

References

[1] Visser C., Kamperman T., Karbaat L., Lohse D., Karperien M., 2018, Sci. Adv., vol. 4, eaao1175

[2] Jiang J., Shea G., Rastogi P., Kamperman T., Venner C. H., Visser C. W., 2021, Adv. Mater., vol. 33, 2006336

[3] Planchette C., Petit S., Hinterbichler H., Brenn G., 2018, Phys. Rev. Fluids, vol. 3, 093603

[4] Baumgartner D., Bernard R., Weigand B., Lamanna G., Brenn G, and Planchette C., 2020, J. Fluid Mech., vol. 885, A23

[5] Baumgartner D., Brenn G, and Planchette C., 2022, J. Fluid Mech., vol. 937, R1

[6] Baumgartner D., Brenn G, and Planchette C., 2022, Int. Multiphase Flow, vol. 150, 104012

[7] Al-Dirawi K., Al-Ghaithi K., Sykes T., Castrejón-Pita J., Bayly A., 2021, J. Fluid Mech., vol. 927, A9

[8] Finotello G., Padding J. T., Deen N. G., Jongsma A., Innings F., Kuipers J. A. M., 2017, Phys. Fluids, vol. 29, 067102.

[9] Stone H.A., Leal L.G., 1989, J. Fluid Mech., vol. 198, 399-427

[10] Rayleigh Lord, 1892, Phil. Mag., vol. 534, 59-70

[11] Stelter M., Brenn G., Yarin A. L., Singh R. P., Durst F., 2000, J. Rheol., vol. 44, 595-616